Atmos. Chem. Phys. Discuss., 12, 12685–12714, 2012
www.atmos-chem-phys-discuss.net/12/12685/2012/
doi:10.5194/acpd-12-12685-2012

Atmospheric Chemistry and Physics Discussions

Mineral dust variability in central West Antarctica associated with ozone depletion

M. Cataldo[1], H. Evangelista[1], J. C. Simões[2], R. H. M. Godoi[3], I. Simmonds[4], M. H. Hollanda[5], I. Wainer[6], F. E. Aquino[2], and R. van Grieken[7]

[1]LARAMG, Universidade do Estado do Rio de Janeiro (Uerj), Pav. Haroldo L. Cunha/Subsolo, Rua São Francisco Xavier 524, Maracanã, 20550-013 Rio de Janeiro, RJ, Brazil
[2]Centro Polar e Climático, Instituto de Geociências, UFRGS, Av. Bento Goncalves 9500, Postal Code 91501-970, Porto Alegre, RS, Brazil
[3]Environmental Engineering Department, Federal University of Paraná (UFPR), Postal Code 19011, 81531-990, Curitiba, PR, Brazil
[4]School of Earth Sciences, University of Melbourne, 3010, Victoria, Australia
[5]Instituto de Geociências, Universidade de São Paulo (USP), Rua do Lago 562, 05508-080, São Paulo, SP, Brazil
[6]Departamento de Oceanografia Física, IO, Universidade de São Paulo USP, Praça do Oceanográfico 191, 05508-120, São Paulo, SP, Brazil
[7]Micro and Trace Analysis Centre, Department of Chemistry, University of Antwerp, 2610, Antwerp, Belgium

Received: 17 November 2011 – Accepted: 1 May 2012 – Published: 21 May 2012

Correspondence to: M. Cataldo (cataldomarcio@gmail.com)

Published by Copernicus Publications on behalf of the European Geosciences Union.

ACPD

12, 12685–12714, 2012

Mineral dust variability in central West Antarctica

M. Cataldo et al.

Abstract

Here we show that mineral dust retrieved from an ice core in the central West Antarctic sector, spanning the last five decades, provides evidence that northerly air mass incursions into Antarctica, tracked by dust microparticles, have slightly declined. This result contrasts with dust in ice core records reported in West/coastal Antarctica, which show significant increases to the present day. We attribute that difference, in part, to changes in the regional climate regime triggered by the ozone depletion and its consequences for the polar vortex intensity. The vortex maintains the Antarctic central region relatively isolated from mid-latitude air mass incursions with implications to the intensification of the Westerlies and to a persistent positive phase of the Southern Annular Mode. We also show that variability of the diameter of insoluble microparticles in central West Antarctica can be modeled by linear/quadratic functions of both cyclone depth (energy) and wind intensity around Antarctica.

1 Introduction

Since 1980 the ozone depletion area in the Antarctic stratosphere has exceeded 1 million km^2 and has been recognized as a threat, with dire implications to marine life (Malloy et al., 1997), increase of skin cancer (Abarca and Casiccia, 2002) and with repercussions for biogeochemical processes in the Antarctic environment (Zepp et al., 1998). Heterogeneous reactions between HCl and $ClONO_2$ and $H_2O + ClONO_2$, involving ozone, were proposed mechanisms to explain observations of stratospheric ozone levels (Solomon et al.,1986). A key factor involved in the catalytic cycle of depletion is attributed to the chlorofluorocarbons (CFC), an anthropogenic molecule, firstly announced in the 1930s. Important players in the destruction of ozone are the polar stratospheric clouds (PSCs) (Solomon, 1999), although controversial (Müller, 2009), and the greenhouse gas emissions that warm the Earth's surface but cool the stratosphere radiatively, a critical factor since chemical reactiveness of ozone is highly sensitive to lowering temperatures (Shindell et al., 1998). Recently, it has been argued that the ozone depletion has climatological consequences (Arblaster and Meehl, 2006; Arblaster et al., 2011). Stratospheric cooling due to ozone depletion may strengthen the Antarctic circumpolar vortex during the Austral spring season. This is consistent with the observed downward trends in tropospheric geopotential height and air temperature (Keeley et al., 2007), which suggests a propagation of this influence to lower levels. The relative cooling of the Antarctic stratosphere contrasts with a warming surrounding troposphere attributed to the greenhouse gas emissions. This thermal gradient strengthens the westerly jets (Thompson et al., 2000), as well as the Westerlies at the surface. The exceptional warming of the Antarctic Peninsula can be seen as a probable consequence of the stronger Westerlies (Delworth et al., 2006) and of more advection of marine moisture and heat flux from the South Pacific Ocean. Recent estimates of the Antarctic surface air temperature distribution, derived from a diverse range of sources such as meteorological ground stations, radiosonde sounding profiles, geochemical proxies in ice cores, statistical methods of data extrapolation, and satellite measurements, have highlighted a near-dipole thermal trend structure over Antarctica, with warming over West Antarctica, contrasting to slightly decreasing (and nearly stable) climatological conditions over central and East Antarctica (Steig et al., 2009; O'Donnell et al., 2011). Marked differences are also observed in sea ice trends since the beginning of the satellite era in 1979, showing increases in the Ross Sea and reductions in the Bellingshausen and Amundsen Seas. In part, such differences have been attributed to the non-annular atmospheric circulation change induced by the stratospheric ozone depletion that strengthens autumn winds around the continent, deepening the Amundsen Sea Low through flow separation around the high coastal orography (Turner et al., 2009). In addition to predictions from numerical models and trends in meteorological databases, evidence of climate changes in Antarctica can be also provided by the interpretation of geochemical proxies retrieved from ice cores and from the very few long-term aerosol monitoring programs. Interpretations of dust deposits in Antarctic ice cores have been connected to atmospheric transport strength

ACPD
12, 12685–12714, 2012

and source availability of dust in the surrounding continents (Basile et al., 1997; Li et al., 2010). At least two recent ice coring projects conducted in West Antarctica revealed the impact of the increasing Westerlies on dust dispersion and deposition on to the Antarctic ice sheet. Projects conducted at James Ross Island (JRI)/northeast Antarctic Peninsula (McConnell et al., 2007) and at Marie Byrd Land (MBL) (Dixon et al., 2011) have both revealed pronounced increases of dust concentrations during the ozone depletion decades. Aluminosilicate levels recorded at JRI more than doubled during the 20th century, with a notable increase after the 1950s, concomitant to increasingly westerly winds and a widespread desertification in Argentine Patagonian semi-desert (McConnell et al., 2007). A similar behavior was observed at MBL, employing the $nssCa^{2+}$ as terrigenous proxy of northerly air mass incursions (Dixon et al., 2011). In the latter work, the authors examined 19 ice cores, most of them in West Antarctica. They suggested that the increases during recent decades were unprecedented for at least the last 200 yr, coinciding with anthropogenically-driven climate changes, such as the greenhouse effect and ozone depletion. It also has been demonstrated that Subantarctic cyclones are very efficient systems at transporting particulate materials to the Antarctic continent (Law et al., 1992), and their effectiveness in dust dispersion is related to their energy and radius (Evangelista and Pereira, 2002). Previous research that utilized tracers of crustal origin as ^{222}Rn and aluminum microparticles (Evangelista and Pereira, 2002) and lead, barium and indium (Burn-Nunes at el., 2011) demonstrated the importance of the cyclones migrating near latitude 60° S in the delivery of warmer air parcels, mineral dust and pollutants to Antarctica. Simmonds et al. (2003) have demonstrated, via trajectory analyses, the atmospheric transport mechanisms involving each of the Southern Hemisphere continents towards Antarctica. During the migration of cyclones around Antarctica, the zonal wind structure is affected by the cyclone vorticity that enhances the meridional wind component, driving warmer dust-enriched air masses to the south. An example of this process is well illustrated by dust plumes displacements observed over the South Atlantic and Southern Ocean by remote sensing (Gasso et al., 2010).

Ice core data interpretation combined with atmospheric dispersion models has improved the understanding of mineral dust reaching Antarctica. For the glacial-interglacial time scales, the atmospheric transport of dust microparticles from Patagonian to Antarctica (with increase in glacial dust flux of approximately 25-fold) resulted in a combined effect of longer lifetime of atmospheric aerosols in the upper troposphere due to a reduced existing hydrological cycle during the ice ages and the extension of South American desert and semi-desert dust sources (Lambert et al., 2008). Models have shown that dust transport towards Antarctica during the last glacial maximum (LGM) was faster for Patagonia than for Australia and southern Africa, while during the last glacial inception, atmospheric transport to Antarctica did not differ significantly from the present (Krinner and Genthon, 2003). For the modern epoch, modeling approaches have revealed that the transport of Patagonian dust to Antarctica is essentially derived from the San Julian's Great Depression region, located inside the semi-desert domain (Li et al., 2010). They have estimated that dust microparticles transport to West Antarctica is a rapid mechanism that takes about 4–5 days. Another potential dust source in South America can be the Bolivian Altiplano (Prospero et al., 2002), as deduced from the Total Ozone Mapping Spectrometer (TOMS) sensor on the Nimbus 7 satellite. Its present-day dust activity sources are attributed to Late Pleistocene lakes that filled vast areas of the Altiplano. Dust resuspended from the Altiplano is mainly sedimentary in origin, mixed with recent accumulations of volcanic eruptions.

In this work we present an analysis of insoluble microparticles retrieved from the Mount Johns (MJ) ice core (79.55° S, 94.23° W), with a view to investigating the incursion of mineral dust to west-central Antarctica during the ozone depletion evolution period. The location of Mount Johns is particularly valuable in this respect, as that site receives air mass influences from both East and West Antarctica, according to surface wind streamlines patterns proposed by Parish and Bromwich (2007). To support our analyses and interpretation, we have derived a number of aspects of the Subantarctic atmospheric circulation and cyclone characteristics since 1958.

2 Methodology

2.1 Ice core retrieval and (radio) isotopic analysis

Drilling was conducted at MJ/central West Antarctica in December 2007 making use of an electro-mechanical drill with a maximum extraction depth of 160 m. The top 40m-ice core, of 9 cm of diameter, was divided into 45 segments ranging from 85 to 95 cm in the field, where density measurements were performed. The MJ ice core was maintained frozen (–20 °C) until laboratory analyses started in Rio de Janeiro State University, Brazil. Sub-sampling was conducted aiming to determinate the deuterium/hydrogen (D/H) ratios, gamma radioactivity and elemental/molecular microanalysis by SEM-EDX (Scanning Electron Microscopes–Energy-dispersive X-ray spectroscopy), as described below.

In clean laboratory conditions, an external layer of the core was removed with a TEFLON knife and the 45 core segments were all cut into slices of 10 cm. The slices were separated into individual vials and melted at 4 °C. Sub-samples of 5 mL were taken for stable isotope analysis. Subsequently, the rest of each ice core segment was mixed in a beaker (cleaned with detergent followed by acid solution), comprising a volume of approximately 2 l per section. Each volume was filtered through a 0.1 µm Nuclepore polycarbonate membrane. The 40m-ice core of MJ was dated by D/H annual variability. Extractions were carried out on a fully automated chromium reduction furnace at 900 °C (H/Device) directly connected to the dual inlet system of an IRMS (DELTAplus Advantage, Thermo Scientific, Germany) equipment. Aliquot of 1 µl from each unknown (liquid) sample was used to determine its D/H ratio. Thirty-five samples were routinely run during a period of 22 h in a sequence with international water reference standards (V-SMOW, SLAP2 and GISP2) in order to check analytical reproducibility and/or anomalous instrumental drift.

Each filtered sample segment of the ice core was firstly submitted to the non-destructive technique of high resolution gamma spectrometry. We used an extended energy range co-axial hyperpure germanium (HPGe) detector with relative efficiency of 20 % and resolution of 2.5 keV at the ^{137}Cs energy peak. This detector is placed inside a 5-ton lead shield, ensuring a very low background. Detector efficiency was obtained using a liquid solution containing a cocktail of radionuclides – NIST (serial number HV951). The cocktail used in this study included the radionuclides ^{133}Ba, ^{57}Co, ^{139}Ce, ^{85}Sr, ^{137}Cs, ^{54}Mn, ^{88}Y, and ^{65}Zn. Details of this method are described in Handl et al. (2008). The net gamma ray spectrum was analyzed in the ^{137}Cs energy window, around 662 keV, and integrated counts were subtracted to 24 h background at the same energy window. The chronology of the ice core was confirmed by the detection of ^{137}Cs Chernobyl peak of 1986, coincident to same date inferred by the D/H. A similar marker was previously detected at the South Pole (Dibb et al., 1990).

2.2 Single particle analysis

SEM-EDX sample analyses were performed using a JEOL 6300 Scanning Electron Microscope (JEOL™, Tokyo, Japan) equipped with backscattered and secondary electron detectors and an EDX detection system at University of Antwerp, Belgium. A Si(Li) X-ray detector, coupled to a PGT-system (Princeton Gamma Tech, Princeton, NJ, USA), was employed for acquiring the X-ray spectra. Particles collected in Nuclepore substrates provided good contrast between the backscattered electron signals (BSE) from the particles and those from the substrate. The electron beam scans the samples, and when the measured backscattered electron signal is higher than a pre-set threshold value, a particle is considered to be detected. When the contours of the located particle are ascertained, the morphology (shape factor) and size (geometric equivalent diameter) are determined. The elemental detection limits of the SEM-EDX are around 1 % in mass. The control software localizes the particles from the BSE image and performs an X-ray measurement within each particle. The intensities of the characteristic peaks in the spectra were determined by the top-hat filter method that stresses regions of high grey intensities (van Espen and Janssens, 1992). In all samples, 400 individual particles were analyzed for each filter. Following the SEM-EDX analysis, only those

ACPD
12, 12685–12714, 2012

variables (elements) detected in more than 1 % of the analyzed particles were considered. In our case, they were Na, Mg, Al, Si, P, S, Cl, K, Ca, Ti, V, Cr, Mn, Fe, Ni, Cu, Zn and Pb, including the diameter estimate and the sump (sum of the characteristic lines in the X-ray spectrum). The database of the elemental composition was submitted to a hierarchical cluster analysis, based on Forgy's algorithm (Anderberg, 1973), in order to classify the particles structures. In this method, each particle is a point in a multidimensional space, where each coordinate or dimension is the concentration of an element. Particles that are close to each other or have similarities between them are combined into a new group. This process is continuous and forms new groups, until all particles are combined into subgroups or end-groups presented as dendrograms. The number of final groups is defined using the Akaike criterion, which is based on the relationship between the order of a system and its minimum entropy (Bondarenko et al., 1996; Hoornaert et al., 2004). The 45 samples were analyzed with an instrumental setup of: accelerating voltage of 20 keV, current of 1 nA, X-ray spectrum acquisition time of 20 s, image magnification of 1000 X and range of diameter analyzed 0.7–20 µm. Particles containing the elements Cl, Cr, Cu, Ni, S, W and V corresponded to 2 % of the total. Hierarchical analyses have revealed 34 groups or clusters. The six most abundant clusters occurred in 70 % of the samples. Our results are based on the elements that can be detected by conventional automated SEM-EDX technique, excluding elements with an atomic number lower than 11, such as C, N and O.

2.3 Climate and meteorological databases

The basic aim of this work is to investigate the mineral dust variability (fraction of insoluble dust and diameter) at MJ with respect to changes in the atmospheric circulation, and particularly wind and cyclone dynamics. To undertake this, we make use of both ground-based meteorological data and the NCEP "reanalyses" (Kalnay et al., 1996) for the period 1958–2009. These reanalyses applied modern assimilation procedures to historical data, and provide the most comprehensive and consistent picture of the four-dimensional structure of the global atmosphere over the selected period (Simmonds,

ACPD
12, 12685–12714, 2012

2003). In data-sparse regions, the introduction of new data at a given time into the assimilating model can produce analyses that appear to have jumps or trends. A case in point is the widespread use in analysis schemes of satellite data starting in 1979 (Hines et al., 2000; Simmonds and King, 2004; Bromwich et al., 2007). However, we take the perspective that it is of considerable value to use the NCEP reanalysis prior to this time, as it provides a broader view of the changes that have occurred over the last half century. In our investigation we are particularly interested in Subantarctic cyclone characteristics. In the International Geophysical Year (1957–1958), many radiosonde stations were established around the periphery of the Antarctic continent, taking quality atmospheric soundings at high temporal frequency. In toto these stations are able to provide a good picture of Subantarctic surface cyclone activity, and for this reason we are comfortable, with certain caveats, in using the data back to 1958.

From the 6-hourly NCEP global mean sea level pressure fields, we locate the cyclones using the algorithm of Lim and Simmonds (2007). In addition to finding cyclones, the algorithm also determines the morphological properties of each cyclone it identifies. One of these properties, which is of particular relevance to the present investigation, is the "depth" of a cyclone, which is the difference between the pressure at the edge of the cyclone and the pressure at the center. In the idealized case of symmetric cyclones, this can be written as $1/4(R^2\nabla^2 p)$ (Simmonds et al., 2008), where R is the cyclone radius and p is the mean sea level pressure. This metric provides direct information of the effect of a cyclone on the environment (and possibly the transport of terrigenous tracers), in that it is proportional to the total eddy flux affected by a cyclone (Simmonds and Keay, 2000) and to the total kinetic energy of the cyclone (Simmonds and Keay, 2009), a consideration essential to our argument here.

2.4 Cluster analyses of databases

Considering the wide range of parameters (geochemical and climatic) employed in this work, we have conducted a hierarchical cluster of analyses in order to investigate the similarity level among them. In this case we have used the single linkage algorithm as the agglomerative hierarchical clustering method and the r-Pearson correlation as the similarity measure (Digby and Kempton, 1987). The r-Pearson correlation measure reflects the degree of closeness of objects, defined with the formula $d = 1 - r$, where d is the distance, and $r = Z(x) \cdot Z(y)/n$ is the dot product of the z-scores of the vectors x and y. The z-score of x is constructed by subtracting from x its mean and dividing by its standard deviation. In cluster analyses, the single linkage (or the nearest neighbor) is a method of calculating distances between clusters in a way that the distance between two clusters is defined as the distance between the two closest elements in the two clusters. The result is summarized as a dendrogram that depicts how the clusters are merged hierarchically.

3 Results and discussions

Although mineral dust records in ice cores of West Antarctica have provided evidence of potential climate effects due to ozone depletion, the same has not been recognized for central Antarctica, a region identified as "climatically isolated". Climate changes attributed to the ozone depletion over the Southern Ocean is one of the conclusive topics at the Executive Summary WMO/UNEP – "Scientific Assessment of Ozone Depletion: 2010", prepared by the Scientific Assessment Panel of the Montreal Protocol on Substances that Deplete the Ozone Layer (http://montreal-protocol.org/Assessment_Panels/SAP/ExecutiveSummary_SAP_2010.pdf). Therefore, the parameter "ozone depletion" is assumed here as a potential cause of the recent atmospheric circulation change ongoing around Antarctica during last decades and a factor able to modulate the inflow of mineral dust into Antarctica. Ozone data presented here are measurements taken during October at Halley Bay Antarctic station. At that site observed ozone content was $\sim 30\,\%$ lower in the spring seasons (October) of 1980–1984 than in the springs of 1957–1973 (Solomon et al., 1986). The issue of the seasonality of ozone changes is complex. Further, there is still no clear consensus on which aspect of the seasonality of ozone is the most important. For example, Keeley et al. (2007)

ACPD
12, 12685–12714, 2012
Mineral dust variability in central West Antarctica
M. Cataldo et al.

comment that "stratospheric ozone depletion peaks in October–November, whereas tropospheric trends are largest in December–January, concurrent with maximum ozone changes close to the tropopause". Surface temperatures are most sensitive to ozone loss near the tropopause; therefore, it has been suggested that the observed tropospheric response is forced mainly by ozone depletion in the lower stratosphere. In our samples, 53 % of the total particles counted ($n = 17600$) presented the elements Si, Al, Fe and Ti as main constituents. The method allows differentiating microparticle compositions individually in the sample insoluble fraction. Therefore, our data refer to the "Fraction of insoluble dust microparticles containing enriched AlSi and Fe" ($F_{\text{insoluble dust}}$) with respect to the total detected insoluble microparticles, which exclude all sea salt compounds in the sample. Insoluble elements/compounds detected were Al, Cr, Cu, Fe, Ni, S, Si, Ti, W, V, AlSi, AlTi, AlSi-Cl, AlSi-Fe, AlSi-Mg, AlSi-S, AlSi-Ti, AlSi/FeCl, Fe-Cr, FeSi, FeSi-S, Fe-Cr-W, KCl, SiCl, SiS, SiS Cu, SZn, TiSi, V-Cr, V-Fe, V Cr, Fe W and V Cr Si. Herein, time series for mineral dust were denoted by F_{AlSi} and F_{Fe} (Fig. 1a). In this case insoluble dust microparticles presented similar trends with respect to ozone depletion, mainly after the 1980s decade (Fig. 1b). The observed ozone content at Halley Bay was ∼ 30 % lower in the Antarctic spring seasons (October) of 1980–1984 than in the springs of 1957–1973 (Solomon et al., 1986). Prior to the satellite era, climate reanalyses data for Antarctica should mostly be interpreted as reliable for the summer months window (December, January and February – DJF) (Bromwich et al., 2007). Accordingly, wind data depicted in Fig. 1c pertain only to the austral summer months (DJF) with 1 standard deviation bars. It is clear that inverse trends between NCEP DJF winds around Antarctica (Fig. 1c) and ozone depletion, AlSi and Fe were evidenced.

The mean cyclone depths were calculated for all cyclones in the 50° S–70° S (Fig. 1d) and 30° S–50° S (Fig. 1e) latitude belts. In addition to the DJF data, we preserved the cyclone annual time series in Fig. 1, since the mineral dust microparticles data in the ice core are of annual resolution. Particularly at 50° S–70° S, the increase of cyclone depth is clearly observed. An inspection at Fig. 1d and 1e indicates that cyclone depth

ACPD
12, 12685–12714, 2012

increased significantly after the 1980s, which coincides with ozone depletion evolution. Therefore, mid-to-Subantarctic zones have been experiencing increasing Westerlies combined with increasing cyclone activity. This presents a favorable scenario for mineral dust delivery to the atmosphere surrounding Antarctica.

Additionally, one may observe the similar ascending behavior of cyclone depth (Fig. 1d, e) and the positive phase of the Antarctic oscillation index, AAO (Fig. 1f). The positive phase of AAO index is persistent after the 1980s and is normally associated with the elevation of air temperatures over the Antarctic Peninsula and decrease in most of the other Antarctic regions (Thompson and Wallace, 2000). The AAO index, in its positive phase, also generates more and stronger cyclones at high southern latitudes (Pezza et al., 2008), causing anomalous southward atmospheric heat flux and confining the sea ice closer to the Antarctic continent in the Bellingshausen/Weddell Seas. The AAO index data presented here are an observation-based Southern Hemisphere Annular Mode index (http://www.antarctica.ac.uk/met/gjma/sam.html – last revised in October, 2011). In this definition 12 stations were used to compose the zonal means from 40° S to 65° S. The basic method to achieve these data is outlined in Marshall (2003). The AAO index is considered the dominant mode of atmospheric variability in the Southern Hemisphere (Kidson, 1988; Thompson and Wallace, 2000; Marshall, 2007; Jones et al. 2009; Visbeck, 2009). Several studies have examined the impacts of changes in the AAO with regard to the atmosphere, sea ice and ocean circulation. These are often related to changes in temperature, surface pressure, precipitation and zonal winds from extra-tropical to high latitudes. With the strengthening of the circumpolar vortex and the associated stronger meridional temperature gradient, the zonal (westerly) winds that circle Antarctica intensify, leading to changes in rainfall, sea ice extent and a southern shift in the storm tracks (Hall and Visbeck, 2002; Lefebvre et al., 2004; Gillett et al., 2006; Sen Gupta and England, 2006; Hendon et al., 2007). The intensification of the Westerlies in conjunction with the positive trend of the AAO has been documented in observations, reanalysis and climate models simulations from the mid-1960s to present (Thompson and Solomon, 2002; Gillet and Thompson, 2003;

ACPD
12, 12685–12714, 2012

Marshall, 2003, 2007; Russell et al., 2006; Visbeck, 2009). Russell et al. (2006) discussed how this trend in AAO has increased the westerly winds by about 20 % over the last 20 yr. Böning et al. (2008) discussed how the poleward shift and intensification of the Southern Hemisphere Westerlies result in an increased circulation in the ocean's subpolar meridional overturning cell. This is also discussed in Saenko et al. (2005). The positive phase of the AAO can also be related to changes in the meridional temperature gradient associated with the cooling of the polar lower stratosphere, attributed to ozone depletion. This is accompanied by warming in the tropical upper troposphere, which is related to an increased vertical gradient of the wind in the mid-latitude tropopause region also affecting the tropospheric winds. Furthermore, Pezza et al. (2008) demonstrated that changes in cyclone density and depth are in extreme phase with AAO. Ozone depletion is known to affect the entire Southern Hemisphere, resulting in broadening of the Hadley cell, zonal winds and a poleward extension of the subtropical dry zones (Polvani et al., 2011).

Uncertainty in our knowledge of the spatial variability of meteorological parameters in the region south of 40° S, before ozone depletion occurred (~ 1979), is quite large, and the marine coverage is very seasonally biased. Considering this uncertainty, we support our findings on the basis of the wind intensity of selected weather stations located at (or near) the maritime Antarctica, whose meteorological databases comprise the period before and after 1979. These data are provided by the SCAR-READER at http://www.antarctica.ac.uk/met/READER/surface/stationwind.html. Table 1 encloses data of 22 Antarctic stations with data continuity large enough to accomplish the above requirement. Compiled wind data show enhances in 64 % of the stations after 1979.

Model simulations indicate that the wind increased significantly over the Southern Ocean region after 1979. Nevertheless, closer to the sea ice edge (where most of the stations of in Table 1 are located), increases of wind intensity is expected to be less and not homogeneously distributed. In Fig. 2 we compare wind trends, from ground stations, with the wind variability derived from a model proposed by Lenton et al. (2009) that used the IPSL-CM4-LOOP prognostic 3-D-coupled carbon-climate model. The

ACPD
12, 12685–12714, 2012

Mineral dust variability in central West Antarctica

M. Cataldo et al.

model predictions (of increase/decrease) apparently fail only in the Indian Ocean sector where data from Syowa, Novolazareskaya, Molodeznaja and Mirny exhibit wind increases contrasting to wind decreases predicted by the model. An important point to consider is that the model is particularly robust to comparisons at the north-northeast Antarctic Peninsula, the closest Antarctic sector to Patagonia semi-desert, which is the most probable source region of mineral dust reaching Antarctica.

The reduction of insoluble mineral dust in the central Antarctica atmosphere may have implications on annual snow accumulation. Decreases in accumulation between 1985 and 2001 inferred by the Polar MM5 mesoscale model (Monaghan et al., 2006a) are particularly obvious over the Ronne-Filchner ice shelf, part of Dronning Maud Land and the coastal regions of East Antarctica. The efficiency of dust as cloud condensation nuclei (CCN) has been previously demonstrated in controlled experimental conditions similarly to those found at sites of the Polar Plateau (Monaghan et al., 2006b). Si-enriched microparticles found at MJ were predominantly spherical (Fig. 3a). This type of grain morphology is expected to exist in semi-arid sites (Rodriguez et al., 2009) and reflects the effect of "aeolian weathering" due to successive collisions among grains at the source regions. Time variability of insoluble microparticle diameters shows a significant increase after 1985, ranging from $1.42 \pm 0.12\,\mu m$ to $1.87 \pm 0.35\,\mu m$ (Fig. 3b). The shift to larger dust microparticles in the Antarctic ice sheet was previously found in the Dome C ice core during episodes of more vigorous circulation from the tropics toward Antarctica (Petit et al., 1981).

The dendrogram obtained by the use of the single linkage as the amalgamation algorithm and the r-Pearson correlation as the similarity measure(Fig. 4) does corroborate our hypothesis that ozone depletion modulates the mineral dust inflow to Antarctica (Group 2 in the cluster analyses) and that the microparticle diameter is mainly constrained by wind and cyclone energy around Antarctica (Group 1 in the cluster analyses).

Mean microparticle diameter correlated significantly with cyclone energy (confidence level of 0.05) for a broad latitudinal band enclosing 30° S–70° S, a region that

ACPD
12, 12685–12714, 2012

covers the greatest fraction of dust emissions at Patagonian semi-desert [the northern Patagonia, centered at (44° S, 67° W) and the San Julian's Great Depression, centered at (49° S, 69° W), formed by scattered dry lakes and topographic depressions]. A higher r-Pearson value was obtained for cyclones migrating in the 50° S–70° S belt ($r = +0.62$). Around 26 to 38 % of the diameter variability in MJ can be explained by cyclone depth model over continental dust source regions and the Southern Ocean. Additionally, we used quadratic models to obtain the best fit between wind intensity around Antarctic (using the DJF database) and diameter (d), expressed in microm of insoluble microparticle be $V_{\mathrm{DFJ}}(\mathrm{m\,s^{-1}}) \sim 4.39 + 3.62d - 0.75d^2$. A very similar model was found considering the annual wind database; we found $V_{\mathrm{annual}}(\mathrm{m\,s^{-1}}) \sim 6.00 + 3.03d - 0.65d^2$.

4 Concluding remarks

On long time scales (e.g., Holocene/Last Glacial), previous works (Petit et al., 1981; Deangelis et al., 1987) have inferred the wind strength on the basis of dust concentrations and diameter distributions measured in deep ice cores. These associations are based on empirical relations between the glaciological data and numerical models that may incorporate considerable uncertainties. For the last decades, in contrast, combined climate models, ground-based observations, satellite observation and annually resolved geochemical databases from ice cores have together provided a unique opportunity to improve knowledge to directly associate the climate dynamics at the Antarctic and surrounding continents with dust microparticle sources, their time variability and diameter distribution while deposited in Antarctic ice sheet. This reinforces the important role of the terrigenous tracers as an important avenue to calibrate models.

Our results contrast to recently published West Antarctic ice core dust analyses (McConnell et al., 2007; Dixon et al., 2011) that point to strong dust enhancements from the last century to the present. In light of the results of the present investigation, we may explain these differences (and other aspects of the dust transport) with the aid of the

ACPD
12, 12685–12714, 2012

schematic scenario presented in Fig. 6. Our data show that during the ozone depletion period, dust advection to the central Western Antarctic sector changed from a stable to a reducing deposition pattern. It suggests that climatically driven processes due to ozone depletion may act differently on the Antarctic continental scale, with respect to the atmospheric transport of particulate matter. According to Thompson and Solomon (2002), recent significant tropospheric trends in Antarctica are related to trends in the lower stratospheric polar vortex that may contribute substantially to the observed cooling over eastern Antarctica and the Antarctic Plateau. An example of that is the temperature decline over central and East Antarctica inferred from the Advanced Very High Resolution Radiometer (AVHRR) sensors (using the thermal infrared channel) from 1982–2004. Therefore, a hypothesis in which the polar vortex may act like an "atmospheric barrier", preventing warmer, coastal air from moving in to the continent's interior, based purely on the climatological approach (Thompson and Solomon, 2002) is also confirmed by the dust geochemical composition retrieved from our ice core, which contrasts to trends observed in western/northern Antarctica.

Acknowledgement. We wish to acknowledge the National Council for Research (CNPq), the Brazilian Antarctic Program (PROANTAR) to have supported this project (grant numbers: 556971/2009-4 and 573720/2008-8) and the Brazilian National Institute for Science and Technology (INCT-Criosfera). Parts of the research were made possible by a grant from the Australian Antarctic Science Advisory Committee.

References

Abarca, J. F. and Casiccia, C. C.: Skin cancer and ultraviolet-B radiation under the Antarctic ozone hole: Southern Chile, 1987–2000, Photodermatol. Photo., 18, 294–302, 2002.

Anderberg, M. R.: Cluster Analysis for Applications. Academic Press, New York, 359 pp., 1973.

Arblaster, J. M. and Meehl, G. A.: Contributions of external forcings to southern annular mode trends, J. Climate, 19, 2896–2905, 2006.

Arblaster, J. M., Meehl, G. A., and Karoly, D. J.: Future climate change in the Southern Hemisphere: competing effects of ozone and greenhouse gases, Geophys. Res. Lett., 38, L02701, doi:10.1029/2010GL045384, 2011.

Basile, I., Grousset, F. E., Revel, M., Petit, J. R., Biscaye, P. E., and Barkov, N. I.: Patagonian origin of glacial dust deposited in East Antarctica (Vostok and Dome C) during glacial stages 2, 4 and 6, Earth Planet Sc. Lett., 146, 573–589, 1997.

Bondarenko, I., Treiger, B., van Grieken, R., and van Espen, P.: IDAS: A Windows based software package for cluster analysis, Spectrochim. Acta B, 51, 441–456, 1996.

Böning, C. W., Dispert, A., Visbeck, M., Rintoul, S. R., and Schwarzkopf, F. U.: The response of the antarctic circumpolar current to recent climate change, Nature Geosci., 1, 864–869, 2008.

Bromwich, D. H., Fogt, R. L., Hodges, K. I., and Walsh, J. E.: A tropospheric assessment of the ERA-40, NCEP, and JRA-25 global reanalyses in the polar regions, J. Geophys. Res., 112, D10111, doi:10.1029/2006JD007859, 2007.

Burn-Nunes, L. J., Vallelonga, P., Loss, R. D., Burton, G. R., Moy, A., Curran, M., Hong, S., Smith, A. M., Edwards, R., Morgan, V. I., and Rosman, K. J. R.: Seasonal variability in the input of lead, barium and indium to Law Dome, Antarctica, Geochim. Cosmochim. Acta, 75, 1–20, 2011.

Deangelis, M., Barkov, N. I., and Petrov, V. N.: Aerosol concentrations over the Last Climatic Cycle (160 Kyr) from an Antarctic Ice Core, Nature, 325, 318–321, 1987.

Delworth, T. L., Broccoli, A. J., Rosati, A., Stouffer, R. J., Balaji, V., Beesley, J. A., Cooke, W. F., Dixon, K. W., Dunne, J., Dunne, K. A., Durachta, J. W., Findell, K. L., Ginoux, P., Gnanadesikan, A., Gordon, C. T., Griffies, S. M., Gudgel, R., Harrison, M. J., Held, I. M., Hemler, R. S., Horowitz, L. W., Klein, S. A., Knutson, T. R., Kushner, P. J., Langenhorst, A. R., Lee, H. C., Lin, S. J., Lu, J., Malyshev, S. L., Milly, P. C. D., Ramaswamy, V., Russell, J., Schwarzkopf, M. D., Shevliakova, E., Sirutis, J. J., Spelman, M. J., Stern, W. F., Winton, M., Wittenberg, A. T., Wyman, B., Zeng, F., and Zhang, R.: GFDL's CM2 global coupled climate models. Part I: Formulation and simulation characteristics, J. Climate, 19, 643–674, 2006.

Dibb, J., Mayewski, P. A., Buck, C. F., and Drummey, S. M.: Beta radiation from snow, Nature, 344, 6270, 1990.

Digby, P. G. N., and Kempton, R. A.: Multivariate Analysis of Ecological Communities, 1st Edn., Chapman and Hall, London, 80–86, 1987.

ACPD

12, 12685–12714, 2012

Mineral dust variability in central West Antarctica

M. Cataldo et al.

Dixon, D. A., Mayewski, P. A., Goodwin, I., Marshall, G. J., Freeman, R., Maasch, K. A., and Sneed, S. B.: An ice-core proxy for northerly air mass incursions into West Antarctica, Int. J. Climatol., 31, doi:10.1002/joc.2371, in press, 2011.

Evangelista, H., and Pereira, E. B.: Radon flux at King George Island, Antarctic Peninsula, J. Environ. Radioact., 61, 283–304, 2002.

Gassó, S., Stein, A., Marino, F., Castellano, E., Udisti, R., and Ceratto, J.: A combined observational and modeling approach to study modern dust transport from the Patagonia desert to East Antarctica, Atmos. Chem. Phys., 10, 8287–8303, doi:10.5194/acp-10-8287-2010, 2010.

Gillett, N. P. and Thompson, D. W. J.: Simulation of recent Southern Hemisphere climate change, Science, 302, 273–275, 2003.

Gillett, N. P., Kell, T. D., and Jones, P. D.: Regional climate impacts of the Southern Annular Mode, Geophysics. Res. Lett., 33, L23704, doi:10.1029/2006GL027721, 2006.

Hall, A. and Visbeck, M.: Synchronous variability in the Southern Hemisphere atmosphere, sea ice, and ocean resulting from the annular mode, J. Climate, 15, 3043–3057, 2002.

Handl, J., Sachse, R., Jakob, D., Michel, R., Evangelista, H., Gonçalves, A. C., and Freitas, A. C.: Accumulation of ^{137}Cs in Brazilian soils and its transfer to plants under different climatic conditions, J. Environ. Radioact., 99, 271–287, 2008.

Hendon, H. H., Thompson, D. W. J., and Wheeler, M. C.: Australian rainfall and surface temperature variations associated with the Southern Hemisphere annular mode, J. Climate, 20, 2452–2467, 2007.

Hines, K. M., Bromwich, D. H., and Marshall, G. J.: Artificial surface pressure trends in the Ncep–Ncar reanalysis over the southern ocean and Antarctica, J. Climate, 13, 3940–3952, 2000.

Hoornaert, S., Godoi, R. H. M., and van Grieken, R.: Elemental and single particle aerosol characterisation at a background station in Kazakhstan, J. Atmos. Chem., 48, 301–315, 2004.

Jones, J. M., Fogt, R. L., Widmann, M., Marshall, G. J., Jones, P. D., and Visbeck, M.: Historical SAM Variability. Part I: Century-Length Seasonal Reconstructions, J. Climate, 22, 5319–5345, 2009.

Kalnay, E., Kanamitsu, M., Kistler, R., Collins, W., Deaven, D., Gandin, L., Iredell, M., Saha, S., White, G., Woollen, J., Zhu, Y., Chelliah, M., Ebisuzaki, W., Higgins, W., Janowiak, J., Mo, K. C., Ropelewski, C., Wang, J., Leetmaa, A., Reynolds, R., Jenne, R., and Joseph, D.: The NCEP/NCAR 40-year reanalysis project, B. Am. Meteorol. Soc., 77, 437–471, 1996.

ACPD
12, 12685–12714, 2012

Mineral dust variability in central West Antarctica

M. Cataldo et al.

Keeley, S. P. E., Gillett, N. P., Thompson, D. W. J., Solomon, S., and Forster, P. M.: Is Antarctic climate most sensitive to ozone depletion in the middle or lower stratosphere?, Geophys. Res. Lett., 34, L22812, doi:10.1029/2007gl031238, 2007.

Kerr, R. A.: A single climate mover for Antarctica, Science, 296, 825–826, 2002.

Kidson, J. W.: Interannual variations in the Southern Hemisphere circulation, J. Climate, 1, 1177–1198, 1988.

Krinner, G. and Genthon, C.: Tropospheric transport of continental tracers towards Antarctica under varying climatic conditions, Tellus, 53, 54–70, 2003.

Lambert, F., Delmonte, B., Petit, J. R., Bigler, M., Kaufmann, P. R., Hutterli, M. A., Stocker, T. F., Ruth, U., Steffensen, J. P., and Maggi, V.: Dust-climate coupling over the past 800 000 years from the EPICA Dome C ice core, Nature, 452, 616–619, doi:10.1038/nature06763, 2008.

Law, R., Simmonds, I., and Budd, W. F.: Application of an atmospheric tracer model to high southern latitudes, Tellus, 44B, 358–370, 1992.

Lefebvre, W., Goosse, H., Timmermann, R., and Fichefet, T.: Influence of the southern annular mode on the sea ice–ocean system, J. Geophys. Res., 109, C09005, doi:10.1029/2004JC002403, 2004.

Lenton, A., Codron, F., Bopp, L., Metzl, N., Cadule, P., Tagliabue, A., and Le Sommer, J.: Stratospheric ozone depletion reduces ocean carbon uptake and enhances ocean acidification, Geophys. Res. Lett., 36, L12606. doi:10.1029/2009GL038227, 2009.

Li, F. Y., Ginoux, P., and Ramaswamy, V.: Transport of Patagonian dust to Antarctica, J. Geophys. Res., 115, D18217, doi:10.1029/2009JD012356, 2010.

Lim, E.-P. and Simmonds, I.: Southern Hemisphere winter extratropical cyclone characteristics and vertical organization observed with the ERA-40 reanalysis data in 1979–2001, J. Climate, 20, 2675–2690, 2007.

Liu, J. P., Curry, J. A., and Martinson, D. G.: Interpretation of recent Antarctic sea ice variability, Geophys. Res. Lett., 31, L02205, doi:10.1029/2003GL018732, 2004.

Malloy, K. D., Holman, M. A., Mitchell, D., and Detrich, H. W.: Solar UVB-induced DNA damage and photoenzymatic DNA repair in Antarctic zooplankton, P. Natl. Acad. Sci. USA, 94, 1258–1263, 1997.

Marshall, G. J.: Trends in the Southern Annular Mode from observations and reanalyses, J. Climate, 16, 4134–4143, 2003.

Marshall, G. J.: Half-century seasonal relationships between the Southern Annular Mode and Antarctic temperature, Int. J. Climatol., 27, 373–383, 2007.

McConnell, J. R., Aristarain, A. J., Banta, J. R., Edwards, P. R., and Simoes, J. C.: 20th-Century doubling in dust archived in an Antarctic Peninsula ice core parallels climate change and desertification in South America, P. Natl. Acad. Sci. USA, 104, 5743–5748, doi:10.1073/pnas.0607657104, 2007.

Monaghan, A. J., Bromwich, D. H., and Wang, S.-H.: Recent trends in Antarctic snow accumulation from Polar MM5 simulations, Philos. Trans. R. Soc. A, 364, 1683–1708, 2006a.

Monaghan, A. J., Bromwich, D. H., Fogt, R. L., Wang, S. H., Mayewski, P. A., Dixon, D. A., Ekaykin, A., Frezzotti, M., Goodwin, I., Isaksson, E., Kaspari, S. D., Morgan, V. I., Oerter, H., van Ommen, T. D., van der Veen, C. J., and Wen, J. H.: Insignificant change in Antarctic snowfall since the International Geophysical Year, Science, 313, 827–831, 2006b.

Müller, R.: A brief history of stratospheric ozone research, Meteorol. Z., 18, 3–24, doi:10.1127/0941-2948/2009/353, 2009.

O'Donnell, R., Lewis, N., McIntyre, S., and Condon, J.: Improved methods for PCA-based reconstructions: case study using the Steig et al. (2009) Antarctic temperature reconstruction, J. Climate, 24, 2099–2115, doi:10.1175/2010JCLI3656.1, 2011.

Parish, T. R. and Bromwich, D. H.: Reexamination of the near-surface airflow over the Antarctic continent and implications on atmospheric circulations at high southern latitudes, Mon. Weather Rev., 135, 1961–1973, doi:10.1175/Mwr3374.1, 2007.

Petit, J. R., Briat, M., and Royer, A.: Ice-age aerosol content from East Antarctic Ice Core samples and past wind strength, Nature, 293, 391–394, 1981.

Pezza, A. B., Durrant, T., Simmonds, I., and Smith, I.: Southern Hemisphere synoptic behavior in extreme phases of SAM, ENSO, sea ice extent and Southern Australia rainfall, J. Climate, 21, 5566–5584, 2008.

Polvani, L. M., Waugh, D. W., Correa, G. J. P., and Son, S.: Stratospheric ozone depletion: the main driver of twentieth-century atmospheric circulation changes in the Southern Hemisphere, J. Climate, 24, 795–812, 2011.

Prospero, J. M., Ginoux, P., Torres, O., and Nicholson, S. E.: Environmental characterization of global sources of atmospheric soil dust identified with the Nimbus 7 Total Ozone Mapping Spectrometer (TOMS) absorbing aerosol product, Rev. Geophys., 40, 1002, doi:10.1029/2000RG000095, 2002.

Rodriguez, I., Gali, S., and Marcos, C.: Atmospheric inorganic aerosol of a non-industrial city in the centre of an industrial region of the North of Spain, and its possible influence on the

ACPD
12, 12685–12714, 2012

climate on a regional scale, Environ. Geol., 56, 1551–1561, doi:10.1007/s00254-008-1253-9, 2009.
Russell, J. L., Dixon, K. W., Gnanadesikan, A., Stouffer, R. J., and Toggweiler, J. R.: The Southern Hemisphere westerlies in a warming world: Propping open the door to the deep ocean, J. Climate, 19(24), 6382–6390, 2006.
Saenko, O. A., Fyfe, J. C., and England, M. H.: On the response of the oceanic wind-driven circulation to atmospheric CO_2 increase, Clim. Dynam., 25, 415–426, 2005.
Sen Gupta, A. S. and England, M. H.: Coupled ocean–atmosphere–ice response to variations in the southern annular mode, J. Climate, 19, 4457–4486, 2006.
Shindell, D. T., Rind, D., and Lonergan, P.: Increased polar stratospheric ozone losses and delayed eventual recovery owing to increasing greenhouse-gas concentrations, Nature, 392, 589–592, doi:10.1038/33385, 1998.
Simmonds, I.: Modes of atmospheric variability over the Southern Ocean, J. Geophys. Res., 108, 8078, doi:10.1029/2000JC000542, 2003.
Simmonds, I. and Keay, K.: Mean Southern Hemisphere extratropical cyclone behavior in the 40-year NCEP-NCAR reanalysis, J. Climate, 13, 873–885, 2000.
Simmonds, I. and King, J. C.: Global and hemispheric climate variations affecting the Southern Ocean, Antarct. Sci., 16, 401–413, 2004.
Simmonds, I., Keay, K., and Lim, E.-P.: Synoptic activity in the seas around Antarctica, Mon. Weather Rev., 131, 272–288, 2003.
Simmonds, I., Burke, C., and Keay, K.: Arctic Climate Change as Manifest in Cyclone Behavior, J. Climate, 21, 5777–5796, 10.1175/2008JCLI2366.1, 2008.
Solomon, S.: Stratospheric ozone depletion: a review of concepts and history, Rev. Geophys., 37, 275–316, doi:10.1029/1999RG900008, 1999.
Solomon, S., Garcia, R. R., Rowland, F. S., Wuebbles, D. J.: On the depletion of Antarctic ozone, Nature, 321, 755–758, doi:10.1038/321755a0, 1986.
Steig, E. J., Schneider, D. P., Rutherford, S. D., Mann, M. E., Comiso, J. C., and Shindell, D. T.: Warming of the Antarctic ice-sheet surface since the 1957 International Geophysical Year, Nature, 457, 459–462, doi:10.1038/Nature07669, 2009.
Thompson, D. W. J. and Solomon, S.: Interpretation of recent Southern Hemisphere climate change, Science, 296, 895–899, 2002.
Thompson, D. W. J. and Wallace, J. M.: Annular modes in the extratropical circulation. Part I: Month-to-month variability, J. Climate, 13, 1000–1016, 2000.

Thompson, D. W. J., Wallace, J. M., and Hegerl, G. C.: Annular modes in the extratropical circulation. Part II: Trends, J. Climate, 13, 1018–1036, 2000.

Turner, J., Comiso, J. C., Marshall, G. J., Lachlan-Cope, T. A., Bracegirdle, T., Maksym, T., Meredith, M. P., Wang, Z. M., and Orr, A.: Non-annular atmospheric circulation change induced by stratospheric ozone depletion and its role in the recent increase of Antarctic sea ice extent, Geophys. Res. Lett., 36, L08502, doi:10.1029/2009gl037524, 2009.

van Espen, P. and Janssens, K.: Spectrum evaluation, in: Handbook of X-ray Spectrometry, edited by: van Grieken, R. and Marcowicz, A., Marcel Dekker, New York, 1992.

Visbeck, M.: A Station-Based Southern Annular Mode Index from 1884 to 2005, J. Climate, 22(4), 940–950, 2009.

Zepp, R. G., Callaghan, T. V., and Erickson, D. J.: Effects of enhanced solar ultraviolet radiation on biogeochemical cycles, J. Photochem. Photobiol. B, 46, 69–82, 1998.

Table 1. Trends in surface wind intensity measured in Antarctic stations (maritime region) before and after 1979 (data compiled from the SCAR-READER database).

Weather Station Around Antarctica	Lat.	Long.	Height (m a.s.l.)	Wind intensity ($m\,s^{-1}$) Before 1979	After 1979	Increase (+) Decrease (–)
Bellingshausen	62.2° S	58.9° W	16	14.0 ± 2.2 (68–79)	14.4 ± 2.0 (80–10)	+
Campbell	52.0° S	169.0° E	19	17.4 ± 2.6 (61–79)	16.2 ± 2.5 (80–10)	–
Casey	66.3° S	110.5° E	42	11.9 ± 3.6 (60–79)	13.6 ± 3.9 (80–90)	+
Davis	68.6° S	78.0° E	13	9.9 ± 2.3 (57–79)	11.0 ± 2.4 (80–10)	+
Dumont_Durville	66.7° S	140.0° E	43	20.6 ± 4.3 (56–79)	18.2 ± 3.6 (80–10)	–
Esperanza	63.4° S	57.0° W	13	16.2 ± 6.5 (57–78)	14.7 ± 4.1 (80–10)	–
Faraday/Vernadsky	65.4° S	64.4° W	11	7.6 ± 2.6 (50–79)	8.9 ± 2.5 (80–10)	+
Grytviken	54.3° S	36.5° W	3	8.6 ± 2.0 (59–79)	8.9 ± 1.6 (01–10)	+
Halley	75.5° S	26.4° W	30	13.3 ± 3.4 (57–79)	12.2 ± 2.9 (80–10)	–
Leningradskaja	69.5° S	159.4° E	304	16.3 ± 3.0 (71–79)	15.8 ± 2.9 (80–91)	–
Macquarie	54.5° S	158.9° E	8	17.0 ± 2.8 (48–79)	18.4 ± 2.5 (80–10)	+
Marambio	64.2° S	56.7° W	198	19.5 ± 4.8 (71–79)	17.1 ± 4.0 (80–10)	–
Marsh	62.2° S	58.9° W	10	12.7 ± 2.2 (70–79)	14.8 ± 3.5 (80–10)	+
Mawson	67.6° S	62.9° E	16	21.8 ± 4.2 (54–79)	22.1 ± 4.2 (80–10)	+
McMurdo	77.9° S	166.7° E	24	11.5 ± 2.6 (56–79)	9.8 ± 2.0 (80–10)	–
Mirny	66.5° S	93.0° E	30	22.4 ± 4.7 (56–79)	21.8 ± 4.3 (80–10)	–
Molodeznaja	67.7° S	45.9° E	40	19.8 ± 6.1 (63–79)	20.8 ± 6.2 (80–99)	+
Novolazarevskaya	70.8° S	11.8° E	119	19.8 ± 6.1 (63–79)	20.8 ± 6.2 (80–99)	+
Orcadas	60.7° S	44.7° W	6	12.2 ± 4.3 (56–79)	12.6 ± 2.3 (80–10)	+
Rothera	67.5° S	68.1° W	32	11.3 ± 2.8 (76–79)	12.1 ± 3.0 (80–10)	+
Signy	60.7° S	45.6° W	6	13.8 ± 3.0 (56–69)	14.9 ± 3.0 (84–95)	+
Syowa	69.0° S	39.6° E	21	11.6 ± 3.6 (57–79)	12.9 ± 3.6 (80–05)	+

ACPD
12, 12685–12714, 2012

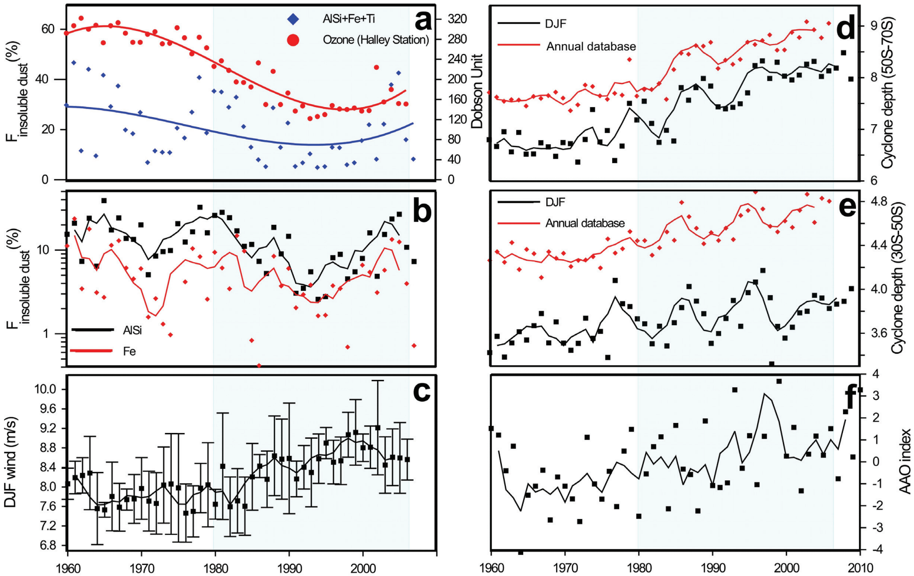

Fig. 1. (a) Fraction of insoluble dust microparticles (AlSi + Fe + Ti) at Mount Johns and ozone concentrations measured for October at Halley Bay Antarctic stations (both with polynomial trends overlaid); **(b)** Fraction of insoluble dust microparticles for AlSi and Fe, individually; **(c)** DJF wind intensity for 40° S–70° S (error bar: 1 standard deviation); **(d)** cyclone depth for DJF and the annual databases for the latitudinal bands 30° S–50° S and **(e)** the same for 50° S–70° S **(e)**; and **(f)** for AAO index. Shaded areas highlight the period of ozone depletion scenario.

ACPD
12, 12685–12714, 2012

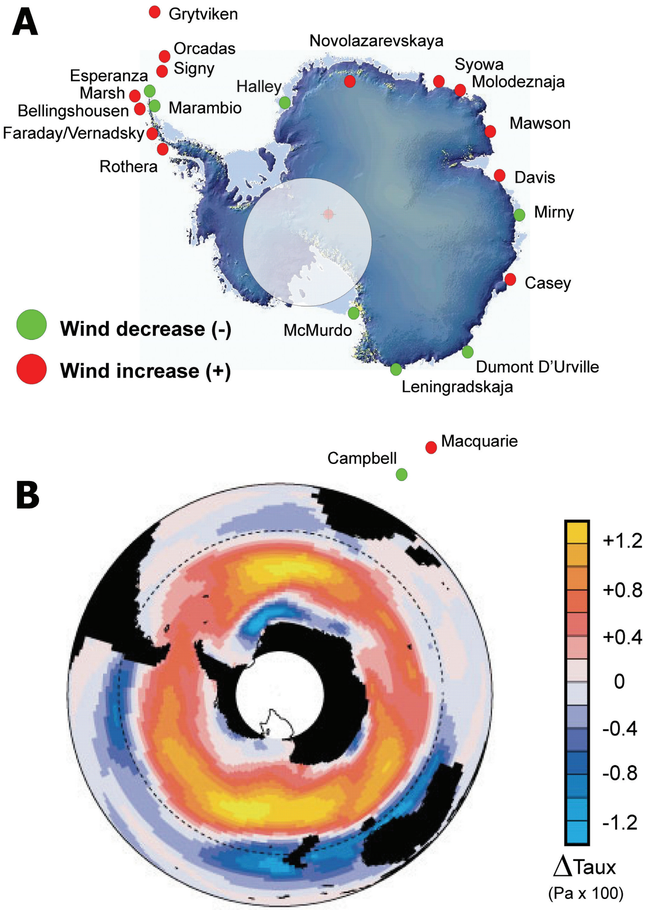

Fig. 2. (A) Surface wind trends, from Antarctic stations, relative to 1979 (see Table 1); and **(B)** for comparison, simulated wind stress over the high-latitude Southern Ocean in a ozone-depletion scenario (Lenton et al., 2009).

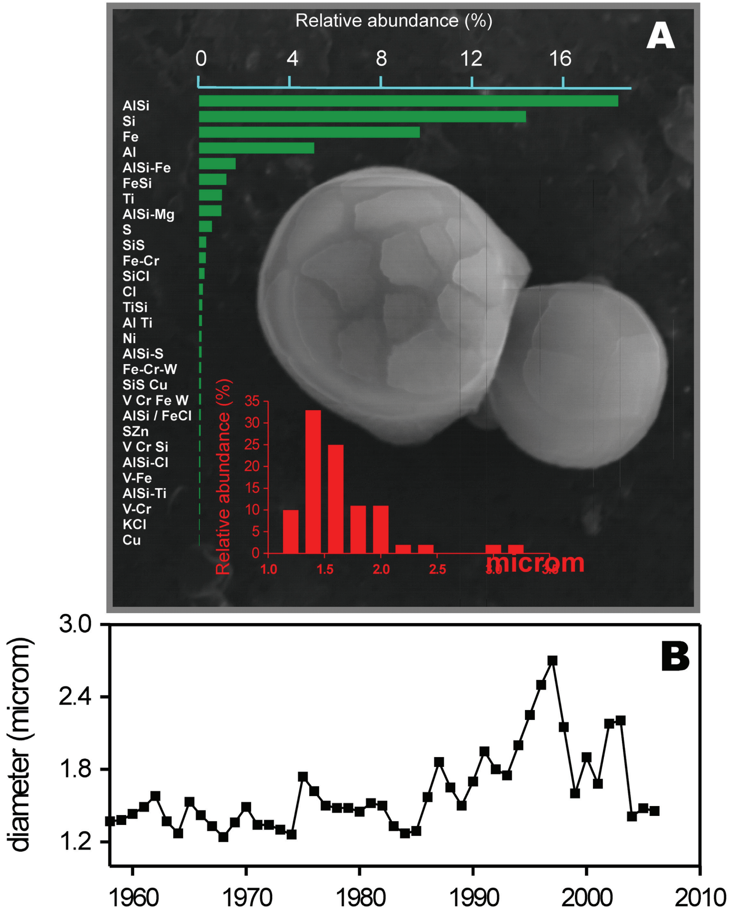

Fig. 3. (A) Size distribution of insoluble microparticles and relative abundance of elements/chemical compounds obtained for Mount Johns ice core (central West Antarctica); **(B)** time variability of microparticle diameters for the same site.

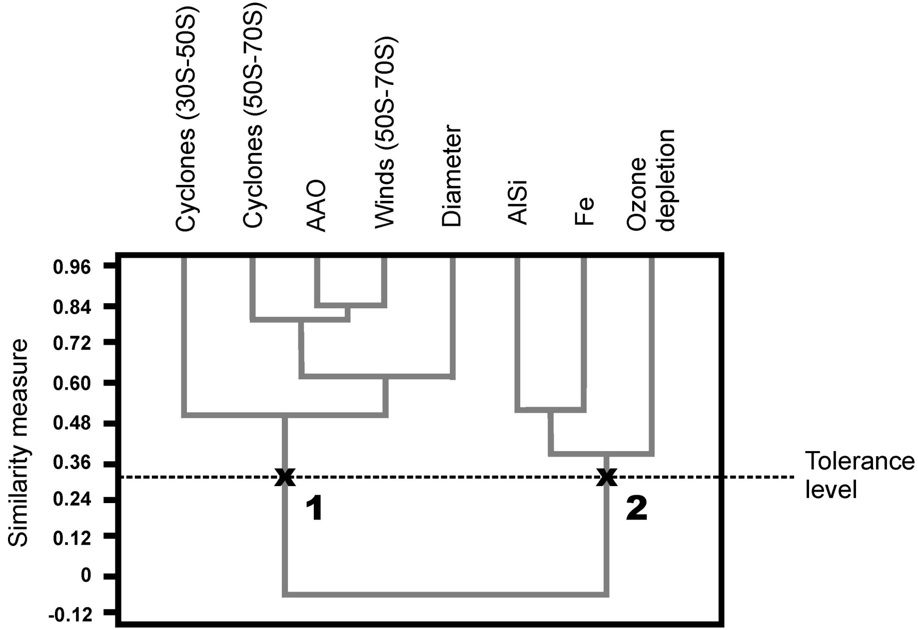

Fig. 4. Dendrogram showing the similarity level among the geochemical and climate parameters. In this case the algorithm used is the single linkage and the r-Pearson correlation was the similarity measure. A tolerance level defined around 0.3 grouped 2 sets of parameters.

ACPD
12, 12685–12714, 2012

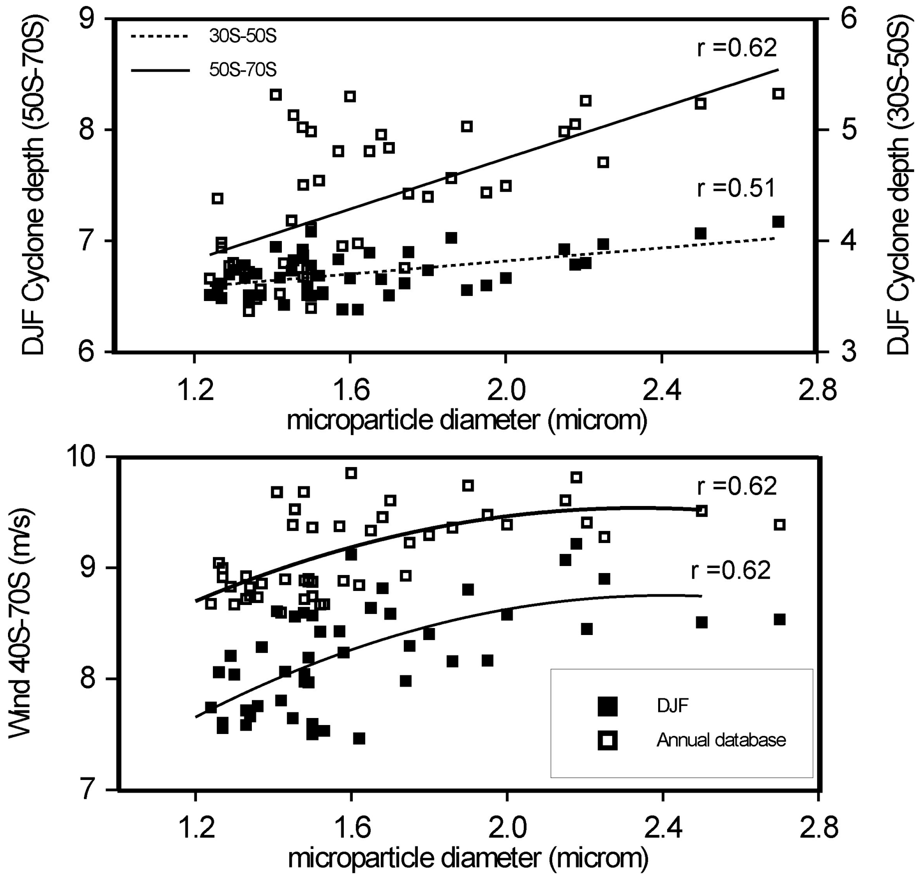

Fig. 5. (upper) Correlation between total insoluble microparticle diameter in Mount Johns ice core and DJF cyclone depth around Antarctica between 1960 and 2007; (bottom) the same of the previous but for wind intensity (40° S–70° S). A quadratic model was used to the best fit of the wind correlation.

ACPD
12, 12685–12714, 2012

Mineral dust variability in central West Antarctica

M. Cataldo et al.

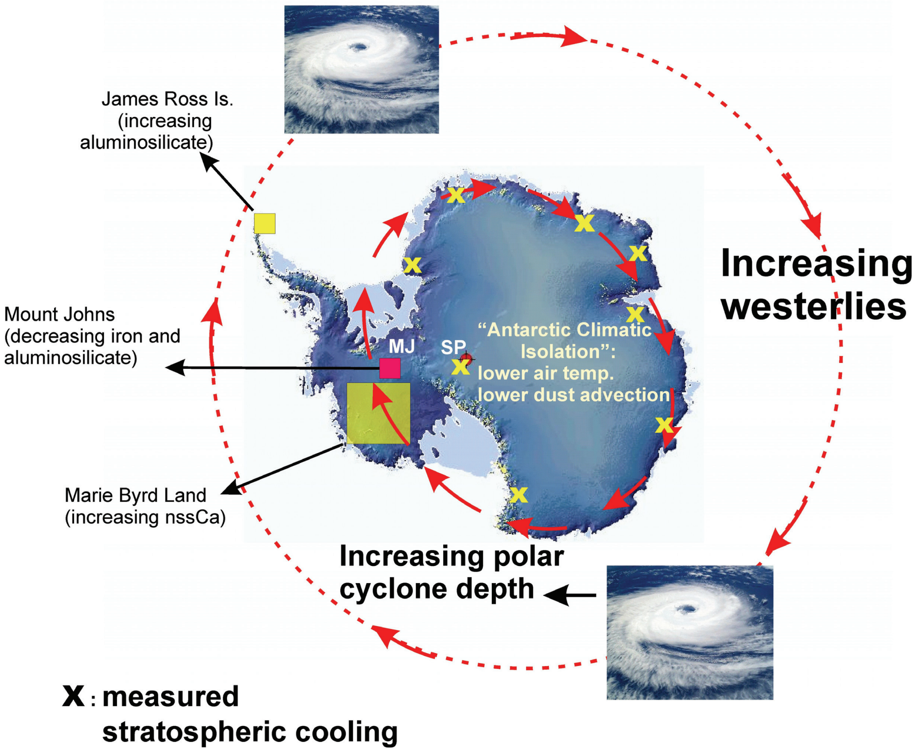

Fig. 6. Schematic summary of recently observed patterns of mineral dust deposition in western Antarctica and continental climate changes driven by the ozone depletion.

ACPD
12, 12685–12714, 2012